Dynamical importance and network perturbations

Ethan Young[1,*] and Mason A. Porter[1,2,3,†]

[1]*Department of Mathematics, University of California,*
Los Angeles, CA, 90095, United States of America
[2]*Department of Sociology, University of California,*
Los Angeles, CA, 90095, United States of America
[3]*Santa Fe Institute, Santa Fe, NM, 87501, United States of America*
(Dated: August 22, 2024)

The leading eigenvalue λ of the adjacency matrix of a graph exerts much influence on the behavior of dynamical processes on that graph. It is thus relevant to relate notions of the importance (specifically, centrality measures) of network structures to λ and its associated eigenvector. We study a previously derived measure of edge importance known as "dynamical importance", which estimates how much λ changes when one removes an edge from a graph or adds an edge to it. We examine the accuracy of this estimate for different network structures and compare it to the true change in λ after an edge removal or edge addition. We then derive a first-order approximation of the change in the leading eigenvector. We also consider the effects of edge additions on Kuramoto dynamics on networks, and we express the Kuramoto order parameter in terms of dynamical importance. Through our analysis and computational experiments, we find that studying dynamical importance can improve understanding of the relationship between network perturbations and dynamical processes on networks.

I. INTRODUCTION

The study of dynamical processes on graphs and other networks is important for many applications, which range from disease spread in populations to the collective behavior of neurons in biological neural networks [1, 2]. A major research direction is the examination of how dynamical processes are affected by network architecture. Consider a network in the form of a graph, in which nodes are connected pairwise (i.e., dyadically) by edges. There is an intimate relationship between a graph's structure and the spectral properties (i.e., the eigenvalues and associated eigenvectors) of its adjacency matrix A (and of other matrices, such as Laplacian matrices) [3].

The leading eigenvalue (i.e., the eigenvalue with the largest magnitude) λ of A determines fundamental properties of many dynamical processes on graphs [2–4]. For example, under certain assumptions, the critical coupling strength for the transition to synchrony in the Kuramoto model [5] of coupled oscillators and in networks of other coupled dynamical systems [6] is proportional to λ. Additionally, $1/\lambda$ gives an estimate of an epidemic threshold for many compartmental models of disease spread on graphs [7]. Relatedly, the percolation threshold for the appearance of a giant component on a graph also involves $1/\lambda$ [8].

In light of the above connections to dynamics, it is relevant to characterize the importances of a graph's nodes and edges using spectral properties of A. Determining the importances (i.e., centralities) of network nodes, edges, and other subgraphs is relevant for ranking and other applications [2], such as removing specific nodes and edges to contain the spread of an infectious disease [9], reach a percolation threshold [10], or minimize congestion in a queueing network [11]. One can express many centrality measures in terms of the leading eigenvector v of A. The prototypical example of such an eigenvector-based centrality is eigenvector centrality [12]. Other eigenvector-based centralities include PageRank [13] and hub and authority scores [14], and generalizations of such centrality measures in multilayer and temporal networks [15–17].

In the present paper, we examine *dynamical importance* [5], which is a centrality measure that gives an estimate of the change in λ due to network perturbations. Using dynamical importance, we compare the effects of edge removals and edge additions (i.e., two different types of network perturbations [18]) on λ for several families of graphs. We then examine network perturbations for the Kuramoto model (which is a system of coupled phase oscillators) on graphs [19]. Under certain assumptions, the Kuramoto model's critical coupling strength, which determines when coupled phase oscillators start to synchronize, is inversely proportional to λ [5].

Our paper proceeds as follows. In Sec. II, we review dynamical importance, compare it to the true change in λ for network perturbations, and discuss its accuracy. In Sec. III, we examine dynamical importance from the perspective of the corresponding change in the leading eigenvector of a graph's adjacent matrix. In Sec. IV, we use dynamical importance to study the effects of network perturbations on a previously derived expression for the order parameter of the Kuramoto model on graphs with approximately-homogeneous degree distributions. Finally, in Sec. V, we conclude and discuss future research directions. In the appendices, we provide a few additional details about some assumptions and other relevant considerations.

In our code repository (see `https://github.com/`

---

* young.j.ethan@gmail.com; now at the Department of Applied Mathematics, University of Washington; ethanjy@uw.edu
† mason@math.ucla.edu

TABLE I. Summary of our key mathematical notation.

Notation	Meaning
Δx	true change in x
δx	first-order approximation of Δx
$\acute{x}$	$x + \Delta x$
$\grave{x}$	$x + \delta x$
$\hat{y}$	quantity computed using Δx
$\check{y}$	quantity computed using δx

ethanjyoung/dynamical_importance.git), we provide software to compute dynamical importance and iteratively add edges with the largest dynamical importance to a graph.

II. DYNAMICAL IMPORTANCE

We begin by reviewing dynamical importance. To aid our presentation, we summarize our key mathematical notation in Table I.

Given a strongly connected graph (i.e., there is a path from each node to each other node) G with adjacency matrix A, leading eigenvalue λ, leading left eigenvector u, and leading right eigenvector v, the dynamical importance [20] of the edge $i \to j$ is

$$\iota_{ij} = \frac{A_{ij} u_i v_j}{\lambda u^T v} \,. \tag{1}$$

Equation (1) arises from the removal or addition of a single edge.

By the Perron–Frobenius theorem for nonnegative matrices [21], the leading eigenvalue λ is real and positive, the entries of u all have the same sign, and the entries of v all have the same sign. Without loss of generality, we take the entries of u and v to be nonnegative. We also assume that (1) the graph G is strongly connected and (2) the graph perturbation has a small effect on λ and its associated eigenvectors for graphs with $N \gg 1$ nodes.

We start by deriving a first-order approximation of the change $[\Delta\lambda]_{ij}$ in λ after the removal or addition of the edge $i \to j$. The eigenvalue equation for the left and right eigenvectors is

$$u^T A v = \lambda u^T v \,. \tag{2}$$

We use perturbation theory to approximate the change in λ for edge removals. Let $A + \Delta A$ denote the new adjacency matrix after the edge removal. Let $\lambda + \Delta\lambda$ denote the associated change in λ, let $u + \Delta u$ denote the change in u, and let $v + \Delta v$ denote the change in v. The eigenvalue equation for the perturbed system is

$$(u + \Delta u)^T (A + \Delta A)(v + \Delta v) = (\lambda + \Delta\lambda)(u + \Delta u)^T (v + \Delta v) \,. \tag{3}$$

We expand (3) and ignore higher-order terms (i.e., terms that are cubic or have higher powers) to obtain

$$u^T \Delta A \, v = \Delta\lambda \, u^T v + \text{higher-order terms} \,. \tag{4}$$

We divide the retained terms by $u^T v$ to isolate $\Delta\lambda$ and obtain

$$\Delta\lambda = \frac{u^T \Delta A \, v}{u^T v} \,. \tag{5}$$

For the removal of the edge $i \to j$, we have

$$[\Delta\lambda]_{ij} = \frac{u_i [\Delta A]_{ij} v_j}{u^T v} \,. \tag{6}$$

Because $[\Delta A]_{ij} = -A_{ij}$, it follows that

$$[\Delta\lambda]_{ij} = \frac{-A_{ij} u_i v_j}{u^T v} \,. \tag{7}$$

We now derive the dynamical importance ι_{ij} of the edge $i \to j$ for edge removals. Consider the relative eigenvalue change

$$\iota_{ij} = \frac{-[\Delta\lambda]_{ij}}{\lambda} \,, \tag{8}$$

where $[\Delta\lambda]_{ij}$ is defined in (7), we have normalized by the leading eigenvalue λ, and the factor -1 ensures nonnegativity. For edge additions, we do not have the factor -1. Inserting (7) into (8) yields

$$\iota_{ij} = \frac{A_{ij} u_i v_j}{\lambda u^T v} \,. \tag{9}$$

Henceforth, we only consider graphs that are undirected and unweighted. For undirected graphs, the subscript ij denotes the bidirectional edge $i \leftrightarrow j$, which necessarily includes both $i \to j$ and $j \to i$. There are two associated 1 entries in the perturbation matrix ΔA. We thus have

$$\iota_{ij} = \frac{u_i v_j + u_j v_i}{\lambda u^T v} \,. \tag{10}$$

The symmetry of A implies that A and A^T have the same eigenvalues, so $u = v^T$. Therefore,

$$\iota_{ij} = \frac{2 v_i v_j}{\lambda v^T v} \,. \tag{11}$$

We refer to ι_{ij} as the "first-order edge dynamical importance" (FoEDI). The eigenvector v has strictly positive
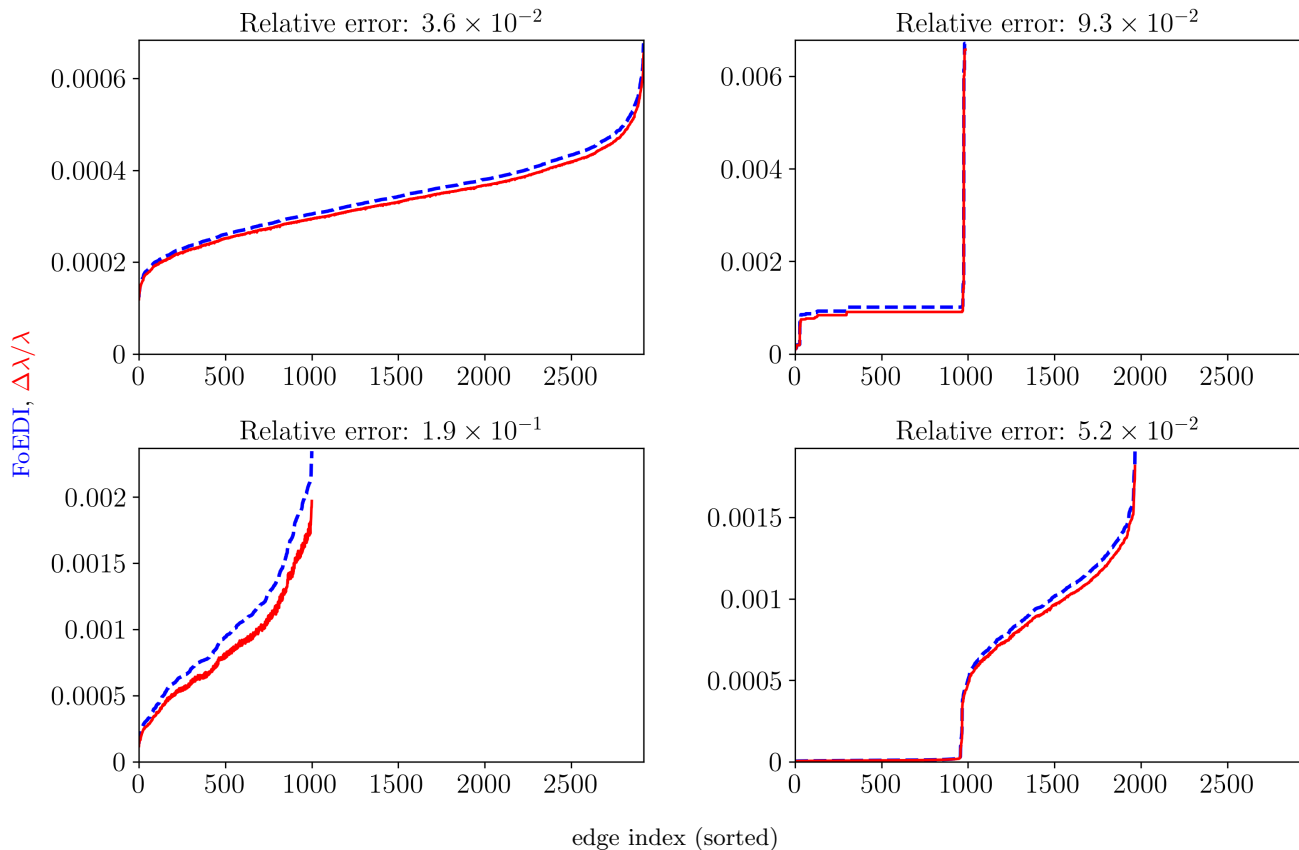
FIG. 1. We show the first-order edge dynamical importance (FoEDI) (dashed blue curve) and $\Delta\lambda/\lambda$ (solid red curve) for edge removals in various 200-node graphs. We order the curves for FoEDI and $\Delta\lambda$ by increasing value of FoEDI. The horizontal axis is the edge index. We plot results for graphs that we construct using (top left) the Erdős–Rényi (ER) model, (top right) the Barabási–Albert (BA) model, (bottom left) the Watts–Strogatz (WS) model, and (bottom right) a stochastic block model (SBM). We describe the parameters of each model in the main text. We use a single instantiation of each type of graph. In each panel, the number of data points equals the number of edges in the associated graph. The relative error is $\|x - y\|_2/\|x\|_2$, where $\|\cdot\|_2$ is the ℓ_2 norm, x is the vector of measured values, and y is the vector of true values.

entries, so $\iota_{ij} > 0$.

One can also use (11) to help select which edge (for edge removals) or non-edge (for edge additions) most increases or most decreases λ. We select one edge at a time, and we use the following procedure (see Algorithm 1) to select edges to add to maximize FoEDI. (We use an analogous procedure to select edges to remove to maximize FoEDI.) Given a graph G with associated adjacency matrix A, the complement graph G^C is a simple [22] graph that consists of all of the edges (except for self-edges) that are not in G. The adjacency matrix A^C of G^C is the complement of A and swaps the 0 entries and 1 entries of A (except for still having 0 values on the diagonal). We compute ι_{ij} for each non-edge of G (i.e., for each edge of G^C) and return the non-edge with the edge index that is associated with the largest ι_{ij}.

Using FoEDI also recovers the Rayleigh quotient $v^T A v / v^T v = \lambda$. See Appendix A for the derivation. This presents opportunities to connect dynamical importance with eigenvalue perturbation theory [23] (e.g., eigenvalue

elasticity). However, many techniques from eigenvalue perturbation theory consider very small perturbations (e.g., changing the weight of an edge in a weighted network), rather than perturbations that change a 1 into a 0 (or vice versa) in one entry of an unweighted adjacency matrix A [24, 25].

A. Comparison to the eigenvalue change $\Delta\lambda$

In Figs. 1 and 2, we compare FoEDI to $\Delta\lambda$ for several graphs. We consider single instantiations of four different types of graphs, which are discussed in detail in the textbook [2]. The first graph is a $G(200, 0.15)$ Erdős–Rényi (ER) graph. The second graph is a Barabási–Albert (BA) graph that we initialize using a single isolated node. The preferential-attachment power is 4, and we add 5 edges at each discrete time step. The third graph is a Watts–Strogatz (WS) graph in which each node is initially adjacent to its $k = 4$ nearest neighbors
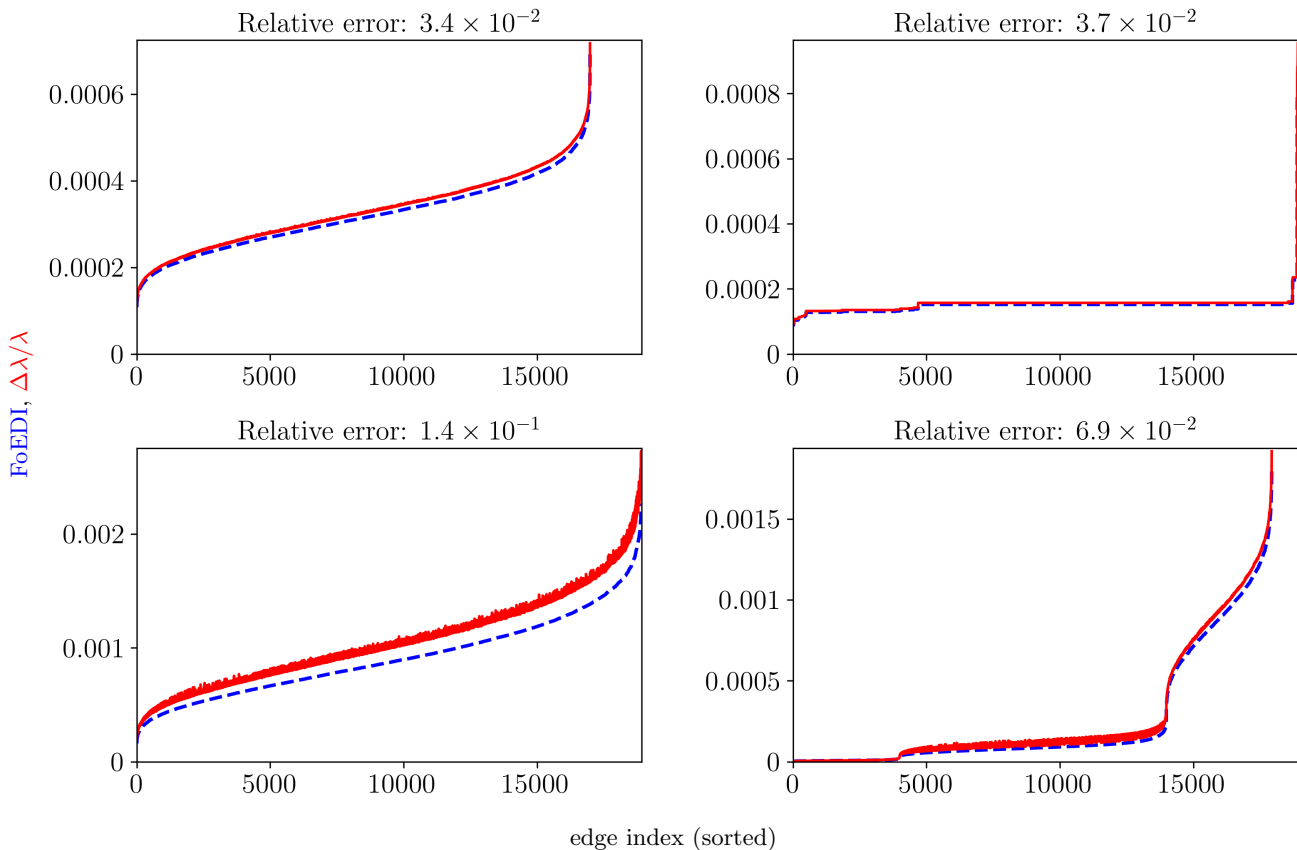
FIG. 2. We show the FoEDI (dashed blue curve) and $\Delta\lambda/\lambda$ (solid red curve) for edge additions. We divide $\Delta\lambda$ by λ to normalize it. We order FoEDI and $\Delta\lambda$ by increasing FoEDI. We show results for (top left) an ER graph, (top right) a BA graph, (bottom left) a WS graph, and (bottom right) an SBM graph. The random-graph realization in each panel is the same as in the corresponding panel of Fig. 1.

Algorithm 1: Adding edges that maximize the first-order edge dynamical importance ι_{ij}.

Input: E^c: the set of edges of the complement graph G^C
Output: G_{complete}: a complete graph

$\iota_G \leftarrow \{\}$
for $k = 1$ **to** $|E^c|$ **do**
    for $e \in E^c$ **do**
        Compute λ, v
        Get indices i, j of e
        Compute $\iota_e = \frac{2v_i A_{ij} v_j}{\lambda v^T v}$
        $\iota_G \leftarrow \iota_e$
    Get indices i, j of $\max(\iota_G)$
    Remove edge e_{ij} from E^c
    Add edge e_{ij} to G
    $\iota_G \leftarrow \{\}$
$G_{\text{complete}} \leftarrow G$
return G_{complete}

---

and the rewiring probability is 0.05. The fourth graph is a stochastic-block-model (SBM) graph with $G(100, 0.2)$ and $G(100, 0.2)$ ER blocks and an independent 0.01 prob-

ability of each edge between nodes in different blocks.

We show our results for edge removals in Fig. 1 and our results for edge additions in Fig. 2. We see that FoEDI always overestimates $\Delta\lambda$ for edge removals and always underestimates $\Delta\lambda$ for edge additions. The difference between FoEDI and the eigenvalue change $\Delta\lambda$ decreases as we increase the numbers of nodes and edges of a graph. In our experiments, this difference is typically negligible. However, this difference is not negligible for additions and removals of nodes. For node dynamical importance, the differences between $\Delta\lambda$ and approximations of it using dynamical importance are significant enough to warrant refining the approximation (e.g., by including second-order terms) to improve its accuracy [26, 27].

As we illustrate in Figs. 1 and 2, FoEDI estimates $\Delta\lambda$ very accurately for some network models (e.g., ER, BA, and SBM graphs), so higher-order approximations will not meaningfully improve accuracy over ι_{ij}. By contrast, FoEDI is noticeably inaccurate in its estimate of $\Delta\lambda$ for our WS graph. Nevertheless, computing FoEDI still provides a helpful estimate even for this example.

We outline a simple, though computationally expensive, edge-addition procedure using FoEDI. In Fig. 3, we
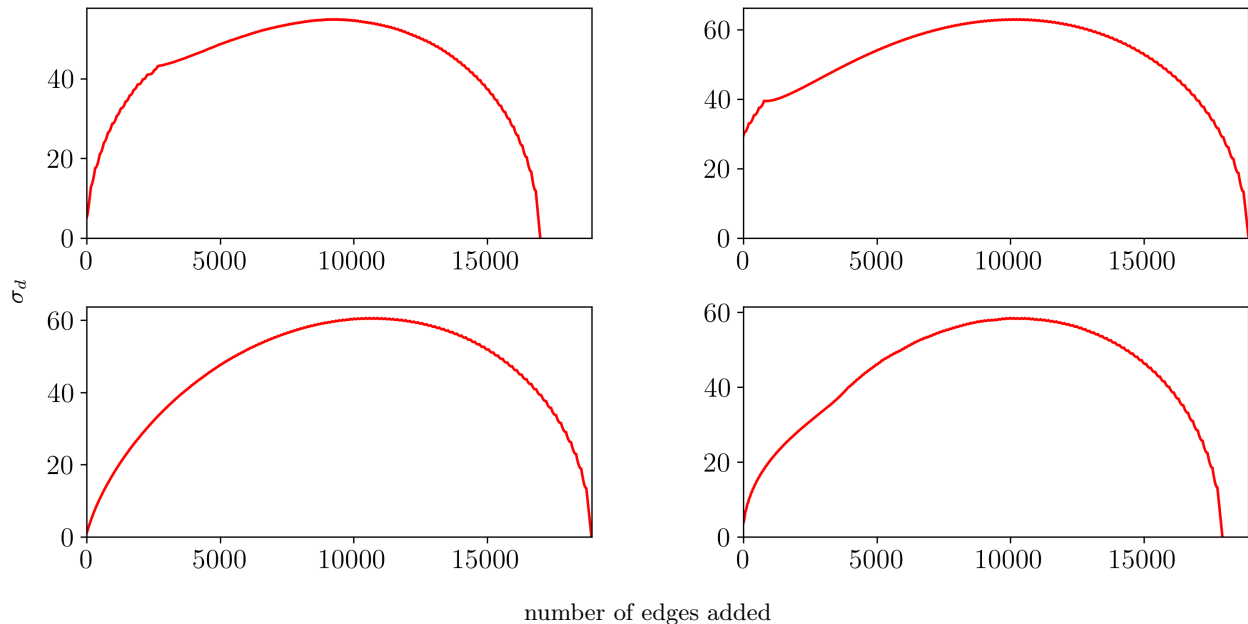
FIG. 3. The standard deviation σ_d of the degree distribution of a graph G as we add edges e_{ij}, one by one, that maximize ι_{ij}. The horizontal axis is the number of edges that we add from the complement graph G^C. We show results for (top left) an ER graph, (top right) a BA graph, (bottom left) a WS graph, and (bottom right) an SBM graph. The random-graph realization in each panel is the same as in the corresponding panel of Fig. 1.

plot the standard deviation σ_d of the graph degree distribution as a function of the number of edges that we add using Alg. 1. In Fig. A.1 in Appendix B, we plot the change in λ as we add edges to each graph. The roughly semicircular curve of σ_d of each graph suggests that initially nodes with large degree tend to accrue edges before other nodes. Subsequently, there is not a clear trend in which nodes have edges added to them. Additionally, it is well-known that $\lambda \leq d_{\max}$, where $d_{\max}$ is the maximum degree of a graph [3].

III. ESTIMATING THE EIGENVECTOR CHANGE Δv

We now derive an approximation of the change Δv in the leading eigenvector of G. Consider the expression for FoEDI in (11), and recall that $u = v^T$ for an undirected graph. The denominator in (11) is constant, so the FoEDI of each edge e_{ij} is determined by the product $v_i v_j$ of the eigenvector entries. Motivated by this product, we examine how much v differs from $v + \Delta v$ by estimating Δv for a graph perturbation.

To approximate Δv, we use the same technique as in our derivation of FoEDI. We begin with the eigenvalue equation

$$Av = \lambda v . \tag{12}$$

We perturb (12) and write

$$(A + \Delta A)(v + \Delta v) = (\lambda + \Delta\lambda)(v + \Delta v) . \tag{13}$$

Expanding (13) and ignoring terms of second and higher order yields

$$Av + A\,\Delta v + \Delta A\,v = \lambda v + \lambda\,\Delta v + \Delta\lambda\,v , \tag{14}$$

which we simplify to obtain

$$\Delta A\,v - \Delta\lambda\,v = \lambda\,\Delta v - A\,\Delta v . \tag{15}$$

Therefore,

$$(\Delta A - \Delta\lambda\,I)v = (\lambda I - A)\Delta v , \tag{16}$$

where I is the $N \times N$ identity matrix. We cannot compute the inverse of $\lambda I - A$ because it is singular. Therefore, we instead compute the Moore–Penrose generalized inverse [28]. Let $\acute{D} = \Delta A - \Delta\lambda I$, and let $D = \lambda I - A$. To compute $\acute{D}$, we use the approximation

$$\iota_{ij}^\dagger = \frac{2v_i v_j}{v^T v} \tag{17}$$

of $\Delta\lambda$. The quantity $\iota_{ij}^\dagger$ is the unnormalized FoEDI.

We seek a first-order approximation δv of Δv. We have

$$(\lambda I - A)\delta v = (\Delta A - \Delta\lambda\,I)v . \tag{18}$$

Solving for δv yields

$$\delta v = D^G \acute{D} v , \tag{19}$$

where D^G denotes the Moore–Penrose generalized inverse of D. In Figs. 4 and 5, we plot the relative error between
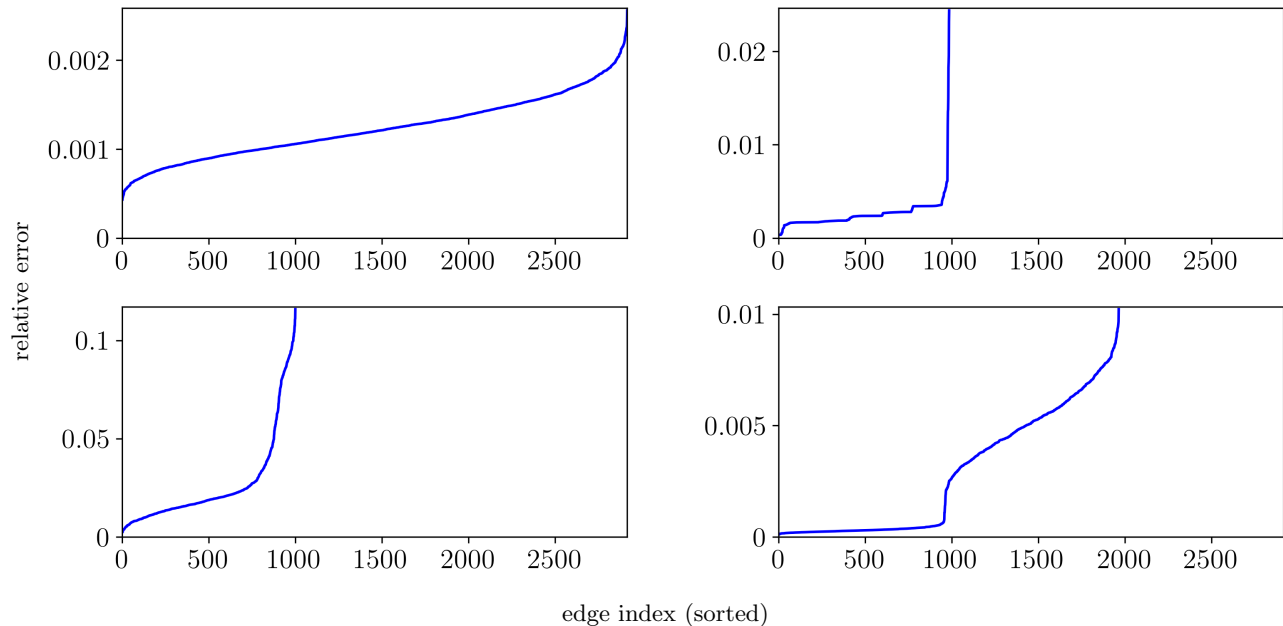
FIG. 4. The relative error between δv and Δv for edge removals. The horizontal axis is the index of the edge, and the vertical axis is the relative error. We order the edge indices by increasing value of the relative error. We show results for (top left) an ER graph, (top right) a BA graph, (bottom left) a WS graph, and (bottom right) an SBM graph. The random-graph realization in each panel is the same in the corresponding panel of Fig. 1.

the approximation δv and the true change Δv for the graphs from Fig. 1. We show our results for edge removals in Fig. 4 and our results for edge additions in Fig. 5. In both figures, the relative error is particularly large for the WS graph.

Computing δv using Eq. (19) is computationally expensive [29], but this expression is useful because we can determine δv for any graph perturbation. We can also use δv to approximate FoEDI after a perturbation. Let $\grave{v}$ denote $v + \delta v$, where we compute δv from Eq. (19). Using Eq. (17), we obtain

$$\grave{\iota}_{ij}^{\dagger} = \frac{2\grave{v}_i \grave{v}_j}{\grave{v}^T \grave{v}} \,. \tag{20}$$

A. Upper bound on Δv

We now discuss an upper bound on Δv. It was derived previously in [27].

Let $\acute{v} = v + \Delta v$, and let λ_2 be the second largest (in magnitude) eigenvalue of A. We have the upper bound [27]

$$\sin(\theta_{v,\acute{v}}) \leq \frac{\|\Delta A\|_2}{\lambda - \lambda_2} \,, \tag{21}$$

where $\theta_{v,\acute{v}}$ denotes the angle between v and $\acute{v}$.

Hultgren [27] noted that the inequality (21) is valid as long as A is symmetric. Because we consider undirected and unweighted graphs, this requirement is satisfied. In

this setting, $\|\Delta A\|_2 = 1$, so we further simplify (21) to obtain

$$\sin(\theta_{v,\acute{v}}) \leq \frac{1}{\lambda - \lambda_2} \,. \tag{22}$$

Based on our observations, which supports a statement in [20], it is often the case that (1) $\lambda - \lambda_2$ is large and (2) it is larger for denser graphs, with $\lambda \to N - 1$ and $\lambda_2 \to -1$ as the number of edges $m \to N(N-1)/2$. However, the bound does not give useful information if λ and λ_2 have similar magnitudes (i.e., if the spectral gap is small). For example, $\lambda - \lambda_2$ can be less than 1 for graphs with community structure (e.g., as generated using an SBM) and ring-like graphs (e.g., as generated using the WS model).

IV. THE KURAMOTO MODEL OF COUPLED OSCILLATORS

The Kuramoto model of coupled phase oscillators is a canonical model to study phenomena such as synchronization on networks [19]. The structure of an underlying network impacts the dynamics of Kuramoto oscillators in interesting ways. We consider the Kuramoto model with diffusive coupling.

We first define the relevant Kuramoto order parameters. The complex-valued "local order parameter" of oscillator i is $r_i e^{\mathrm{i}\psi_i}$, where $\mathrm{i} = \sqrt{-1}$ is the imaginary unit and $r_i \in [0, 1]$ and $\psi_i \in [-\pi, \pi)$, respectively, are the
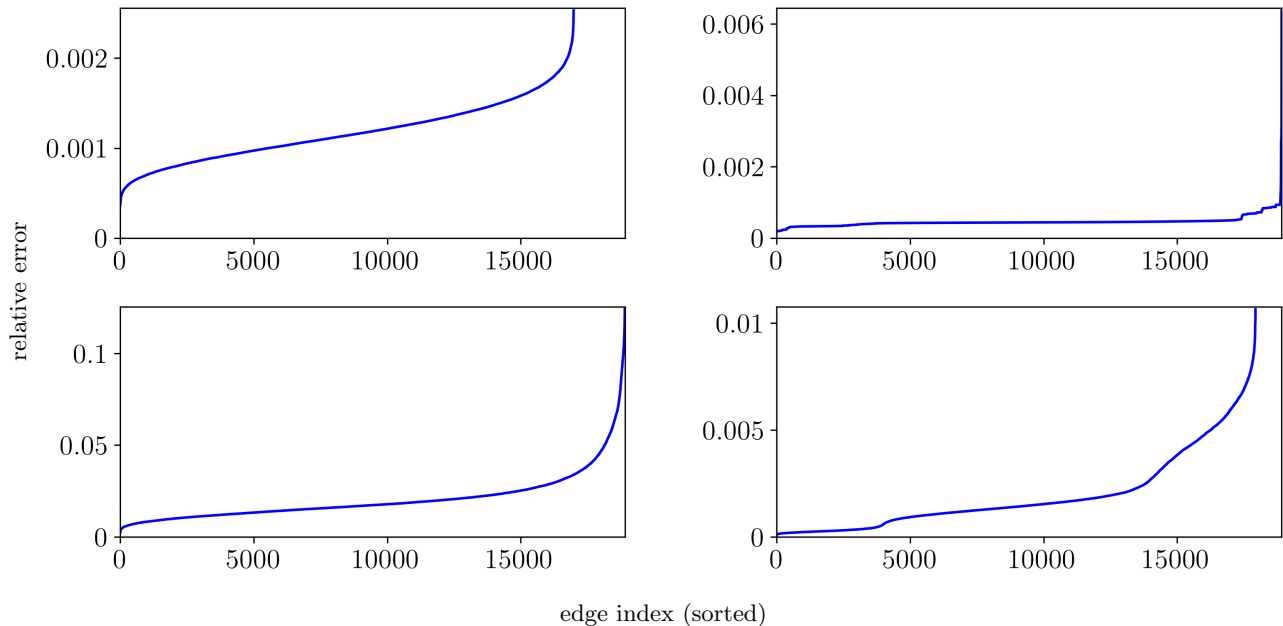
FIG. 5. The relative error between δv and Δv for edge additions. The horizontal axis is the index of the edge, and the vertical axis is the relative error. We order the edge indices by increasing value of the relative error. We show results for (top left) an ER graph, (top right) a BA graph, (bottom left) a WS graph, and (bottom right) an SBM graph. The random-graph realization in each panel is the same as in the corresponding panel of Fig. 1.

amount of synchrony and the mean phase of oscillator i and its neighbors. We use the positive real-valued order parameter $r = |\frac{1}{N} \sum_{i=1}^{N} r_i e^{i\psi_i}|$ to measure the overall amount of synchrony of all oscillators.

Given the phase $\Theta_i(t)$ of oscillator i, its natural frequency ω_i, and the coupling strength k, the Kuramoto model on a graph is the set of coupled ordinary differential equations

$$\dot{\Theta}_i = \omega_i + k \sum_{j=1}^{N} A_{ij} \sin(\Theta_j - \Theta_i). \qquad (23)$$

The critical coupling strength k_c signifies the onset of a transition to synchronization [19]. Under specific assumptions (see Appendix C), which include the requirement that ω_i is statistically independent of r_i and ψ_i, it has been shown that $k_c \propto 1/\lambda$ [5]. Specifically, under those assumptions, the $N \to \infty$ asymptotic expression for k_c is

$$k_c = \frac{2}{\pi \lambda g(0)} \,, \qquad (24)$$

where $g(\omega)$ is the probability distribution from which we draw the natural frequencies. Let

$$\eta = \frac{\langle v \rangle^2 \lambda^2}{N \langle d \rangle^2 \langle v^4 \rangle} \qquad (25)$$

and

$$\alpha = \frac{-g''(0)}{8g(0)} \,, \qquad (26)$$

where $\langle d \rangle$ denotes the mean degree of a graph. The square of the order parameter is

$$r^2 = \left(\frac{\pi^2 g(0)^2 \eta}{4\alpha} \right) \left(\frac{k}{k_c} - 1 \right) \left(\frac{k}{k_c} \right)^{-3} . \qquad (27)$$

Restrepo et al. [5] made several assumptions (see Appendix C) to ensure that Eqs. (24) and (27) are valid. They noted that graphs with an approximately-homogeneous degree distribution (specifically, graphs for which the mean degree $\langle d \rangle \approx \lambda$) guarantee that Eq. (27) holds asymptotically and illustrated numerically that Eq. (27) is valid for $k/k_c \lesssim 1.3$. Accordingly, we work in this setting.

A. Estimating the order parameter r with edge additions

Because of the presence of λ and v in Eqs. (24) and (25), we can study how r changes as we add edges to a graph, provided the degree distribution remains approximately homogeneous. Using our estimates of $\Delta\lambda$ in Eq. (17) and Δv in (19), we obtain perturbed versions of Eqs. (24) and (25) after adding the edge e_{ij} to a graph G. These expressions are

$$\hat{k}_c = \frac{2}{\pi(\lambda + \Delta\lambda)g(0)} \qquad (28)$$

and

$$\hat{\eta} = \frac{\langle \acute{v} \rangle^2 (\lambda + \Delta\lambda)^2}{N(\langle d \rangle + \Delta\langle d \rangle)^2 \langle \acute{v}^4 \rangle}, \qquad (29)$$

where $\acute{v} = v + \Delta v$.

Using Eqs. (28) and (29), the square of the order parameter after adding the edge e_{ij} is

$$\hat{r}^2 = \left(\frac{\pi^2 g(0)^2 \hat{\eta}}{4\alpha} \right) \left(\frac{k}{\hat{k}_c} - 1 \right) \left(\frac{k}{\hat{k}_c} \right)^{-3}. \qquad (30)$$

Therefore, for a fixed coupling strength k, we see that $\hat{r}^2 > r^2$ for edge additions. An analogous derivation gives $\hat{r}^2 < r^2$ for edge removals.

We illustrate Eq. (30) with a particular scenario. Consider a graph with $N \gg 1$ nodes such that the degree d_i of each node i satisfies $N \geq d_i \gg 1$ and the mean degree satisfies $\langle d \rangle \approx \lambda$. When we add an edge, the leading eigenvalue λ and the mean degree $\langle d \rangle$ all increase by small amounts. Therefore, $\hat{\eta} \approx \eta$ and $\hat{k}_c < k_c$, so $\hat{r}^2 > r^2$ for edge additions.

We now relate r to FoEDI. The expression $\pi^2 g(0)^2 \hat{\eta}/(4\alpha)$ in Eq. (30) approximately equals $\pi^2 g(0)^2 \eta/(4\alpha)$ because $\hat{\eta} \approx \eta$ for a graph with an approximately-homogeneous degree distribution. Let $\beta = \pi^2 g(0)^2 \eta/(4\alpha)$, which is a constant. Substituting β
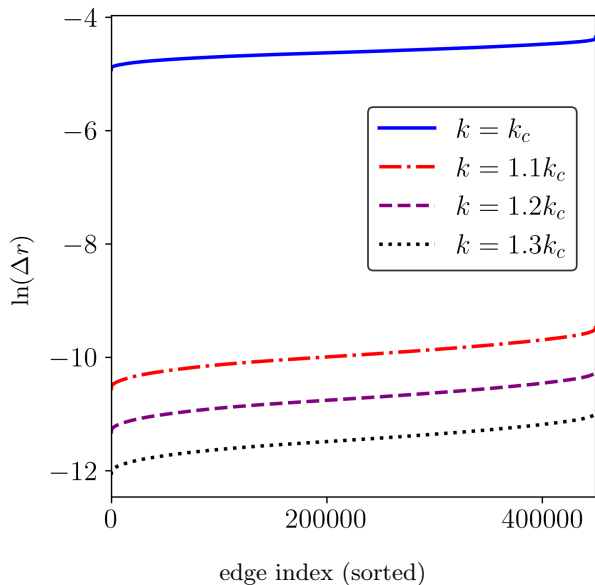

FIG. 6. The natural logarithm of the order-parameter change Δr for each edge e_{ij} of the complement graph G^C in order of increasing values of Δr. The horizontal axis is the edge index after we sort the edges. We describe the graph structure and model parameters in the main text. The solid blue curve gives Δr for the critical coupling strength $k = k_c$, the dash-dotted red curve gives Δr for the coupling strength $k = 1.1k_c$, the dashed purple curve gives Δr for $k = 1.2k_c$, and the dotted black curve gives Δr for $k = 1.3k_c$.

and Eq. (28) into Eq. (30) yields

$$\hat{r}^2 = \beta \left(\frac{k}{\hat{k}_c} - 1 \right) \left(\frac{k}{\hat{k}_c} \right)^{-3}$$

$$= \beta \left(\frac{k\pi(\lambda + \Delta\lambda)g(0)}{2} - 1 \right) \left(\frac{k\pi(\lambda + \Delta\lambda)g(0)}{2} \right)^{-3}. \qquad (31)$$

Let $\gamma = \pi g(0)/2$, which is also a constant. We use the unnormalized FoEDI $\iota_{ij}^{\dagger}$ as a first-order estimate of $\Delta\lambda$ for each edge e_{ij}. Substituting γ and $\iota_{ij}^{\dagger}$ into Eq. (31) yields

$$\check{r}^2 = \beta \left(k\gamma(\lambda + \iota_{ij}^{\dagger}) - 1 \right) \left(\gamma(k\lambda + \iota_{ij}^{\dagger}) \right)^{-3}. \qquad (32)$$

Equation (32) expresses the approximate squared order parameter $\check{r}^2$ after an edge perturbation in terms of the coupling strength k and the unnormalized FoEDI $\iota_{ij}^{\dagger}$. As we discussed in Sec. IIA, the way that one adds edges to a graph can break the approximate homogeneity of a degree distribution. That is, edge additions can cause the standard deviation of the degree distribution to become too large. We do not know an upper bound on the number of edges that one can add and still preserve approximate degree-distribution homogeneity, although one can obtain an approximate bound numerically on a case-by-case basis. We expect that the maximum standard deviation of the degree distribution that retains degree-distribution homogeneity increases with the graph size (i.e., the number of nodes) N.

We give an example that demonstrates how to use Eq. (32). As in [5], we suppose that the distribution of the natural frequencies is $g(\omega) = (3/4)(1 - \omega^2)$ for $-1 < \omega < 1$ and $g(\omega) = 0$ otherwise. We consider a graph with $N = 1000$ nodes and use a configuration model (which is a type of random-graph model) [30] without self-edges or multi-edges. The method that we use to prevent self-edges and multi-edges is described in [31]. We choose the node degrees uniformly at random from the set $\{75, 76, \ldots, 124, 125\}$. For each edge e_{ij} of the complement graph G^C, we compute Eq. (17) and insert it into (32). We consider coupling strengths of $k = k_c$, $k = 1.1k_c$, $k = 1.2k_c$, and $k = 1.3k_c$; equation (27) is valid for these values.

In Fig. 6, we plot $\ln(\Delta r) = \ln(\acute{r} - r)$ for the different coupling strengths k for a single instantiation of our configuration-model graph. For this graph, $\lambda \approx \langle d \rangle$, so its degree distribution is approximately homogeneous. We observe that Δr is smaller for larger multiples of the critical coupling strength k_c. This observation is expected, because the order parameter r for the critical coupling strength $k = k_c$ (i.e., when the oscillators begin to synchronize) increases more due to an edge addition than when $k > k_c$. For progressively larger values of k, an individual edge addition has a progressively smaller impact on the order parameter. For $k = 1.3k_c$ in our example, adding edges uniformly at random is comparably effective as adding edges that maximize FoEDI.

V. CONCLUSIONS AND DISCUSSION

We studied a previously derived measure of edge importance called dynamical importance, which is a first-order approximation of how much the leading eigenvalue λ of a graph's adjacency matrix A changes when one removes an edge from it or adds an edge to it [32]. We examined first-order edge dynamical importance (FoEDI) for undirected, unweighted graphs. We investigated several computational aspects of FoEDI and related it to diffusive Kuramoto dynamics on graphs. We compared FoEDI to the true change in λ, derived an approximation of the change in the leading eigenvector v after a graph perturbation, and expressed the Kuramoto order parameter in terms of FoEDI.

We compared FoEDI to the true change $\Delta\lambda$ in λ for Erdős–Rényi (ER) graphs, Barabási–Albert (BA) graphs, Watts–Strogatz (WS) graphs, and stochastic-block-model (SBM) graphs. In our computations, we observed larger relative errors for our WS graph than for the other graphs. We also constructed an edge-addition scheme using FoEDI and observed that large-degree nodes tend to accrue edges earlier than other nodes.

We derived a first-order estimate δv of the true change Δv of an adjacency matrix's leading eigenvector v after a graph perturbation. Our estimate is computationally infeasible for large graphs, as it involves computing a generalized inverse of a matrix. Nevertheless, its small relative error for some graphs, such as those that are generated by the ER and BA random-graph models, demonstrates its potential usefulness. We also discussed a previously derived upper bound on the angle between v and $v + \Delta v$ for any graph perturbation. We observed that this bound does not give useful information for graphs with small spectral gaps. Interesting future directions to explore include (1) examining the numerical stability of computing generalized inverses of relevant adjacency matrices and (2) exploring how to exploit symmetries and other structures of adjacency matrices to yield better bounds on δv. Although removing an edge from A or adding an edge to it corresponds to changing two entries of A for an undirected graph (and to one entry for a directed graph), one cannot use methods like the Sherman–Morrison formula [33] to update the adjacency-matrix inverse because the leading eigenvalue λ also changes. To efficiently compute a generalized inverse X^G of a matrix X, it seems useful to explore iterative methods that are numerically stable when X is nonsingular [34, 35].

We also estimated the change in the order parameter r (which measures the amount of synchronization) in a Kuramoto coupled-oscillator model after edge additions. We focused on an expression for r for graphs with approximately-homogeneous degree distributions (i.e., when λ approximately equals the mean degree). In this setting, we derived an expression for the change $\check{r}$ in r in terms of FoEDI. Studying perturbations of r in this manner is efficient and practical because one only needs

to compute the eigendecomposition of A. Although computing FoEDI grants flexibility in estimating the change in the order parameter for any edge, adding too many edges can break the approximate degree-distribution homogeneity. Our exploration suggests that it may be useful to study the relationship between network perturbations and synchronization. One relevant research direction is to study the number of edges that one needs to add (for different edge-addition strategies) to a network of Kuramoto oscillators to achieve global synchrony [36–38].

It is common to study the relationship between network perturbations and dynamical processes on networks in the context of controllability of dynamics on graphs (and on more complicated types of networks) [39]. We expect that edge-perturbation and node-perturbation schemes that are based on dynamical importance are particularly relevant in situations (e.g., in diffusive dynamics) in which spectral information plays a role in determining the behavior of a dynamical process. An important avenue of research involves exploring how dynamics are affected by directed edges and weighted edges (e.g., see [40]). For instance, one can examine how the perturbations of edge weights (i.e., increasing or decreasing edge weights, without removing or adding any edges) impact the dynamics of a system. These perturbations are different than our paper's perturbations (which are sometimes called "modifications" [24, 25] or "network surgery" [41] because of their finite size for finite-size networks), as they can be infinitesimal in size.

Appendix A: Recovering the Rayleigh quotient with FoEDI

In this appendix, we relate FoEDI to the Rayleigh quotient. Consider an undirected and unweighted graph with adjacency matrix A. Expanding Eq. (1) yields

$$\iota_{ij} = \frac{u_i A_{ij} v_j + u_j A_{ji} v_i}{\lambda u^T v} . \tag{A1}$$

The leading eigenvalue λ is a normalization factor in Eq. (A1), so we ignore it and look at the unnormalized FoEDI

$$\iota_{ij}^\dagger = \frac{u_i A_{ij} v_j + u_j A_{ji} v_i}{u^T v} . \tag{A2}$$

We begin with the sum of $\iota_{ij}^\dagger$ over all edges. This sum is

$$\sum_{i=1}^{N} \sum_{j=1}^{N} \iota_{ij}^\dagger = \sum_{i=1}^{N} \sum_{j=1}^{N} \frac{A_{ij} u_i v_j + A_{ji} u_j v_i}{u^T v} . \tag{A3}$$
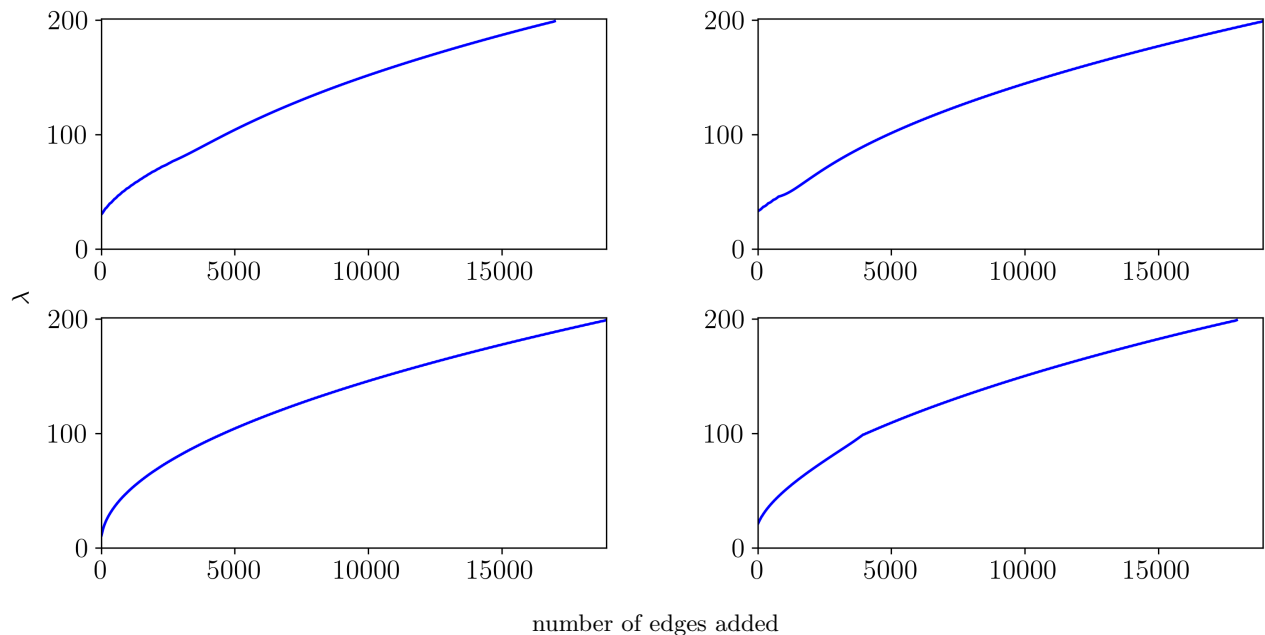
FIG. A.1. The leading eigenvalue λ (vertical axis) as we add edges e_{ij}, one by one, that maximize the FoEDI ι_{ij}. The horizontal axis is the number of edges that we add from the complement graph G^C. We show results for (top left) an ER graph, (top right) a BA graph, (bottom left) a WS graph, and (bottom right) an SBM graph. The random-graph realization in each panel is the same in the corresponding panel of Fig. 1.

It follows that

$$\sum_{i=1}^{N}\sum_{j=1}^{N} \iota_{ij}^{\dagger} = \frac{u^T A v}{u^T v} \, . \qquad (A4)$$

The right-hand side of (A4) is the Rayleigh quotient. Because A is symmetric, $u^T = v$, so we obtain

$$\sum_{i=1}^{N}\sum_{j=1}^{N} \iota_{ij}^{\dagger} = \lambda \, . \qquad (A5)$$

Appendix B: Calculation of the leading eigenvalue λ as we add edges

In Fig. A.1, we show how λ changes as we add edges e_{ij} that maximize ι_{ij} to a graph G. The nonlinear increase in λ as a function of the number of added edges is consistent with how σ_d (the standard deviation of the degree distribution) changes in Fig. 3 as one adds more edges. We expect the slope of λ to be large when the slope of

σ_d is large. Our numerical computations confirm this expectation.

Appendix C: The assumptions on the critical coupling strength k_c and the order parameter r

We now outline the assumptions that were made in [5] to obtain Eqs. (24) and (27).

The assumptions to obtain Eq. (24) are as follows:

(i) the graph G is unweighted and undirected;

(ii) the distribution $g(\omega)$ is symmetric about a local maximum (which, without loss of generality, we take to be at $\omega = 0$);

(iii) the degree d_i of each node $i \in \{1, \ldots, N\}$ satisfies $d_i \gg 1$; and

(iv) the existence of solutions r_i (i.e., the positive real-valued order parameter of oscillator i and its neighbors) and ψ_i (i.e., the mean phase of oscillator i and its neighbors) are statistically independent of ω_i.

The assumptions to obtain Eq. (27) are as follows: (i) $k \approx k_c$ and (ii) $\langle d^4 \rangle$ is finite.

[1] M. A. Porter and J. P. Gleeson, *Dynamical Systems on Networks: A Tutorial*, Frontiers in Applied Dynamical Systems: Reviews and Tutorials, Vol. 4 (Springer Inter-

national Publishing, Cham, Switzerland, 2016).

[2] M. E. J. Newman, *Networks*, 2nd ed. (Oxford University Press, Oxford, UK, 2018).

[3] P. Van Mieghem, *Graph Spectra for Complex Networks*, 2nd ed. (Cambridge University Press, Cambridge, UK, 2023).

[4] N. Masuda, M. A. Porter, and R. Lambiotte, Random walks and diffusion on networks, Physics Reports **716**, 1 (2017).

[5] J. G. Restrepo, E. Ott, and B. R. Hunt, Onset of synchronization in large networks of coupled oscillators, Physical Review E **71**, 036151 (2005).

[6] J. G. Restrepo, E. Ott, and B. R. Hunt, Emergence of synchronization in complex networks of interacting dynamical systems, Physica D: Nonlinear Phenomena **224**, 114 (2006).

[7] Y. Wang, D. Chakrabarti, C. Wang, and C. Faloutsos, Epidemic spreading in real networks: An eigenvalue viewpoint, in *Proceedings of the 22nd International Symposium on Reliable Distributed Systems* (2003) pp. 25–34.

[8] B. Bollobás, C. Borgs, J. Chayes, and O. Riordan, Percolation on dense graph sequences, The Annals of Probability **38**, 150 (2010).

[9] J. T. Matamalas, A. Arenas, and S. Gómez, Effective approach to epidemic containment using link equations in complex networks, Science Advances **4**, eaau4212 (2018).

[10] Y. Gao, S. Chen, J. Zhou, H. Stanley, and J. Gao, Percolation of edge-coupled interdependent networks, Physica A: Statistical Mechanics and its Applications **580**, 126136 (2021).

[11] F. Ying, A. O. G. Wallis, M. A. Porter, S. D. Howison, and M. Beguerisse-Díaz, Minimizing congestion in single-source, single-sink queueing networks, SIAM Journal on Applied Mathematics **83**, 1832 (2023).

[12] P. Bonacich, Factoring and weighting approaches to clique identification, Journal of Mathematical Sociology **2**, 113 (1972).

[13] S. Brin and L. Page, The anatomy of a large-scale hypertextual Web search engine, Computer Networks and ISDN Systems **30**, 107 (1998).

[14] J. M. Kleinberg, Authoritative sources in a hyperlinked environment, Journal of the ACM **46**, 604 (1999).

[15] D. Taylor, S. A. Myers, A. Clauset, M. A. Porter, and P. J. Mucha, Eigenvector-based centrality measures for temporal networks, Multiscale Modeling & Simulation: A SIAM Interdisciplinary Journal **15**, 537 (2017).

[16] M. Wu, S. He, Y. Zhang, J. Chen, Y. Sun, Y. Liu, J. Zhang, and H. Poor, A tensor-based framework for studying eigenvector multicentrality in multilayer networks, Proceedings of the National Academy of Sciences of the United States of America **116**, 15407 (2019).

[17] D. Taylor, M. A. Porter, and P. J. Mucha, Tunable eigenvector-based centralities for multiplex and temporal networks, Multiscale Modeling & Simulation: A SIAM Interdisciplinary Journal **19**, 113 (2021).

[18] Some authors pointedly refer to such as perturbations as "modifications" because these changes are of finite size, rather than asymptotically small, for graphs of finite size [24, 25].

[19] F. A. Rodrigues, T. K. D. Peron, P. Ji, and J. Kurths, The Kuramoto model in complex networks, Physics Reports **610**, 1 (2016).

[20] J. G. Restrepo, E. Ott, and B. R. Hunt, Characterizing the dynamical importance of network nodes and links, Physical Review Letters **97**, 094102 (2006).

[21] C. D. Meyer and I. Stewart, *Matrix Analysis and Applied Linear Algebra*, 2nd ed. (Society for Industrial and Applied Mathematics, Philadelphia, PA, USA, 2023).

[22] A "simple" graph is an unweighted, undirected graph with no self-edges or multi-edges [2].

[23] R. A. Horn and C. R. Johnson, *Matrix Analysis*, 2nd ed. (Cambridge University Press, Cambridge, UK, 2012).

[24] X. Liu., G. Strang, and S. Ott, Localized eigenvectors from widely spaced matrix modifications, SIAM Journal on Discrete Mathematics **16**, 479 (2003).

[25] M. Paton, K. Akartunali, and D. J. Higham, Centrality analysis for modified lattices, SIAM Journal on Matrix Analysis and Applications **38**, 1055 (2017).

[26] A. Milanese, J. Sun, and T. Nishikawa, Approximating spectral impact of structural perturbations in large networks, Physical Review E **81**, 046112 (2010).

[27] N. Hultgren, *Centrality and Network Analysis: A Perturbative Approach to Dynamical Importance*, Honors thesis, Duke University (2011), available at https://dukespace.lib.duke.edu/dspace/handle/10161/3771.

[28] R. Penrose, A generalized inverse for matrices, Mathematical Proceedings of the Cambridge Philosophical Society **51**, 406 (1955).

[29] For an $N \times N$ matrix, computing the Moore–Penrose generalized inverse using the singular-value decomposition (SVD) has complexity $O(N^3)$. However, there exist algorithmic improvements (e.g., that exploit certain matrix structures) that reduce the cost of computing Moore–Penrose inverses. For example, the algorithm in [42] that is based on the full-rank Cholesky factorization has a lower-bound complexity of $O(\log N)$ for symmetric, positive-definite matrices.

[30] B. K. Fosdick, D. B. Larremore, J. Nishimura, and J. Ugander, Configuring random graph models with fixed degree sequences, SIAM Review **60**, 315 (2018).

[31] F. Viger and M. Latapy, Efficient and simple generation of random simple connected graphs with prescribed degree sequence, in *Computing and Combinatorics* (Springer Berlin Heidelberg, Berlin, Heidelberg, 2005) pp. 440–449.

[32] One can also define a notion of dynamical importance that is based on node perturbations [20].

[33] J. Sherman and W. J. Morrison, Adjustment of an inverse matrix corresponding to a change in one element of a given matrix, Annals of Mathematical Statistics **21**, 124 (1950).

[34] V. Y. Pan, F. Soleymani, and L. Zhao, An efficient computation of generalized inverse of a matrix, Applied Mathematics and Computation **316**, 89 (2018).

[35] H. Hotelling, Some new methods in matrix calculation, Annals of Mathematical Statistics **14**, 1 (1943).

[36] A. Townsend, M. Stillman, and S. H. Strogatz, Dense networks that do not synchronize and sparse ones that do, Chaos: An Interdisciplinary Journal of Nonlinear Science **30**, 083142 (2020).

[37] M. Kassabov, S. H. Strogatz, and A. Townsend, Sufficiently dense Kuramoto networks are globally synchronizing, Chaos: An Interdisciplinary Journal of Nonlinear Science **31**, 073135 (2021).

[38] M. Kassabov, S. H. Strogatz, and A. Townsend, A global synchronization theorem for oscillators on a random graph, Chaos: An Interdisciplinary Journal of Nonlinear Science **32**, 093119 (2022).

[39] L. Xiang, F. Chen, W. Ren, and G. Chen, Advances in network controllability, IEEE Circuits and Systems Magazine **19**, 8 (2019).

[40] R. Delabays, P. Jacquod, and F. Dörfler, The Kuramoto model on oriented and signed graphs, SIAM Journal on Applied Dynamical Systems **18**, 458 (2019).

[41] B. Allen, G. Lippner, Y.-T. Chen, B. Fotouhi, N. Momeni, S.-T. Yau, and M. A. Nowak, Evolutionary dynamics on any population structure, Nature **544**, 227 (2017).

[42] P. Courrieu, Fast computation of Moore–Penrose inverse matrices, Neural Information Processing — Letters and Reviews **8**, 25 (2005).